Comparative Study of the Primary Photochemical Mechanisms of Nitric Oxide and Carbonyl Sulfide on Ag(111)

Robert T. Kidd, David Lennon,† and Stephen R. Meech*

School of Chemical Sciences, University of East Anglia, Norwich NR4 7TJ, U.K.

Received: March 17, 1999; In Final Form: June 23, 1999

Detailed studies of the primary photochemical mechanism of two quite different adsorbates, OCS and NO, on a common substrate, Ag(111), have been made. Irradiation of OCS on Ag(111) at wavelengths shorter than 500 nm leads to dissociation into CO_g and S_a. For a Ag(111) surface saturated with NO, irradiation at all wavelengths studied results in desorption of both NO and N_2O. The relative photochemical cross sections for the reactions have been measured as a function of the wavelength, polarization, and angle of incidence of the radiation. The polarization dependence was measured at four wavelengths and three angles of incidence, and the results were compared with predictions for both adsorbate and substrate localized excitation mechanisms. The results are similar for both adsorbates and consistent with a substrate excited mechanism. No evidence was found for a change in photochemical mechanism with wavelength for either adsorbate. The wavelength dependence of the photochemical cross sections was studied in greater detail, between 280 and 600 nm. For irradiation at wavelengths shorter than 400 nm, the wavelength dependence is essentially identical for each surface, strongly suggestive of a substrate excited mechanism. For the photodissociation, of OCS a threshold at ca. 500 nm was observed, while for NO desorption, no threshold was detected out to 600 nm. The wavelength-dependent cross sections were modeled assuming the primary photochemical mechanism to be attachment of hot, sub-vacuum electrons generated by substrate absorption. For OCS, the cross section was modeled assuming an adsorbate attachment level at 3.2 eV and a nascent distribution of hot electrons. For NO, at least two adsorbate attachment levels are required to reproduce the data and the effect of secondary hot electrons must be taken into account. It was concluded that all measurements could be interpreted on the basis of the substrate-mediated hot electron attachment mechanism, but that the limited knowledge of adsorbate electronic structure hampered more definitive conclusions.

1. Introduction

The photochemistry of molecules adsorbed on metal surfaces has been discussed in terms of two competing mechanisms.[1] The first involves direct excitation of the adsorbate, or its complex with the surface. The second, which derives from models of desorption induced by electronic transitions (DIET),[2] suggests that photochemistry occurs from a negative ion state formed by attachment of an excited, hot, substrate electron. The hot electron attachment (HEA) mechanism gained considerable credence from studies of the translational and internal energy distributions of the photoproduct,[3] which were well reproduced by theoretical calculations.[4] Once the HEA mechanism is accepted as plausible, it rapidly appeared dominant, since the cross section for optical absorption by a metal substrate is almost always much greater than that of a monolayer of adsorbate.[5] Thus, HEA should win out over direct adsorbate excitation, provided attachment levels of the appropriate energy are available. This last proviso reveals one of the key difficulties in modeling the HEA model—information on the electronic structure of adsorbates above the Fermi level, E_F, and below the vacuum level is sparse. Despite this problem, it has proved possible to invoke the HEA mechanism in a number of cases,[1,3,4] while an unambiguous assignment to adsorbate excitation has proved possible in fewer cases.[6] The distinction has usually been made on the basis of the different wavelength and polarization dependence of the two mechanisms,[6a,7,8] although analysis of the product state distribution can be equally informative.[1,4] A schematic representation of the two mechanisms is shown in Figure 1.

Unfortunately, even in the case of some much studied adsorbates, there remains controversy on the assignment of the primary mechanism of photochemistry. Recently, Ho noted that the wavelength-dependent cross section data for NO photodesorption on a variety of metal substrates could be described by a common curve, rising monotonically with increasing energy (a similar analysis was possible for adsorbed O_2).[9] The easiest interpretation of these observations is that the primary photochemical mechanism is optical excitation on the low-energy edge of an adsorbate localized transition—an adsorbate-mediated mechanism. This is in contradiction to polarization-resolved and product translational energy measurements on the same systems, where the HEA mechanism was invoked.[3,4,10] It can be argued that HEA will also yield a similar monotonic curve, when the effect of secondary electrons, or hot electron cascades, is taken into account.[11,12] However, this necessarily introduces an element of curve fitting, since the substrate optical constants are not identical for the metals concerned.[13]

In this paper, we will present a comparative study of the photochemistry of two different adsorbates (OCS and NO), which undergo quite different photoreactions on a common Ag(111) surface. We will report the wavelength dependence of the photochemical yields and include in the analysis the

* To whom correspondence may be addressed. E-mail: s.meech@uea.ac.uk.

† Present address: Department of Chemistry, University of Glasgow, Glasgow, G12 8QQ, U.K.

10.1021/jp990944e CCC: $18.00
Published on Web 08/13/1999

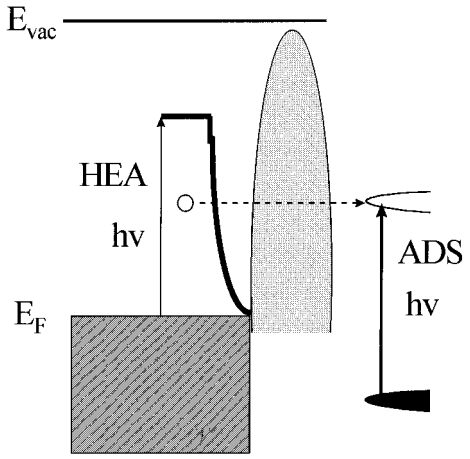

Figure 1. Schematic illustration of the hot electron attachment (HEA) and adsorbate excitation (ADS) models of adsorbate photochemistry. In HEA, hot electrons are generated by substrate absorption of incident radiation, with an energy in excess of the Fermi level (E_F) up to the photon energy. Either nascent or secondary electrons may tunnel through the barrier at the surface to attach to a negative ion state of the adsorbate. In the ADS mechanism, direct excitation of an occupied to vacant electronic state of the adsorbate−substrate complex occurs.

influence of hot electron cascades.[11,12] We will also report the wavelength dependence of the polarization and incident angle resolved photochemical cross sections. Both the adsorbate systems to be discussed here have been studied before. Zhou and White were the first to report the photodissociation of OCS, to CO_g and S_a, on Ag(111),[14] but the two competing mechanisms outlined above could not be distinguished. So et al. made a quite detailed study of the photodesorption of NO from Ag(111) and Cu(111).[7] These authors concluded that a substrate excited mechanism operated at wavelengths longer than 350 nm, but at shorter wavelengths an adsorbate-mediated mechanism could contribute. Where there is overlap between our observations and those of So et al., the agreement is quite good. However, we note that it is now thought that the photoactive species on Ag(111) is the NO dimer.[15] This has some implications for the interpretation of the photochemistry.[16]

The point of the present *comparative* study of two quite different adsorbates on a common substrate is that it should reveal rather unambiguously a common mechanism only if substrate excitation is dominant. With respect to the electronic spectra of these molecules, gaseous OCS has a broad continuous absorption with an onset at 4.5 eV (260 nm), while in the solid state transitions at 4.3 and 4.7 eV (288 and 264 nm) are seen.[14,17] The onset of monomeric NO absorption occurs at 230 nm in the gas phase.[17] The $(NO)_2$ dimer exhibits broad band excitation at around 5.0 eV (250 nm).[18] Even though the onset of absorption for these molecules occurs over a similar energy range, the fact that they interact in different ways with the surface (OCS being more tightly bound than $(NO)_2$, for example), is expected to yield quite different photochemical behavior.

In the following, it will be shown that there are many common features in the photochemistry of these two surfaces, suggestive of a substrate excitation mechanism operating throughout the 280−600 nm region. There are also some differences between the two sets of results, particularly at lower energy, and these are discussed. The results are analyzed in terms of the HEA mechanism. The limitations of the model are discussed, and some other possibilities are mentioned. It should be stated that here we focus mainly on the primary mechanism of photochemistry. The photokinetics of these adsorbates observed under prolonged irradiation reveal some complex features which are discussed elsewhere.[16b]

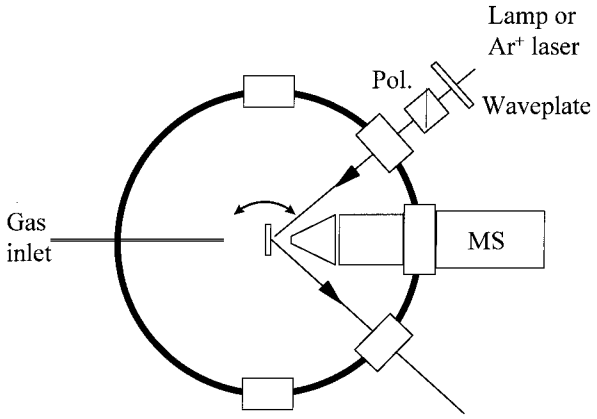

Figure 2. Schematic representation of the experimental apparatus. Radiation was from either a Xe lamp, via a monochromator, or the UV or visible lines of an Ar^+ laser. For laser irradiation, the polarization direction is controlled by a half waveplate. A polarizer is used to ensure either pure s- or p-polarized incident radiation. This is incident on the temperature controlled sample which is held in UHV. The photoproducts are detected by a quadrupole mass spectrometer mounted on a translation stage.

2. Experimental Section

All experiments were performed on a Ag(111) crystal (diameter 10 mm, thickness 3 mm) located at the center of a spherical stainless steel ultrahigh vacuum chamber fitted with fused silica viewports. The crystal was orientated to within ±0.5° of the (111) plane and polished to a roughness of <1 μm. The vacuum chamber was pumped by a 200 L s^{-1} turbo molecular pump and a liquid nitrogen cooled titanium sublimation pump (base pressure of the chamber was 5×10^{-11} Torr). Pressures were measured using an uncorrected ion gauge.

The Ag(111) crystal was mounted onto tungsten rods which were in contact with a liquid nitrogen reservoir. With this arrangement, a base temperature of 82 K was achieved, as measured by a chromel−alumel thermocouple wedged into a spark cut hole in the side of the crystal. The sample could be resistively heated at a fixed rate (typically 2 K s^{-1}). The sample was located at the center of the chamber by translation stages, and the whole Dewar assembly could be rotated to face either the doser or the mass spectrometer. A schematic diagram of the experimental arrangement is shown in Figure 2.

The Ag(111) crystal surface was cleaned by argon ion bombardment (uniform current density over the crystal face of 1 μA cm^{-2}) followed by annealing at 700 K for 1 h. The sample was cooled to 82 K, and the gases were dosed onto the surface via a directional doser located 20 mm from the surface. For both OCS and NO, doses of 1 langmuir were sufficient to yield saturation coverage; neither gas forms multilayers at 82 K.

The source for surface photochemical measurements was either a 100 W xenon arc lamp or a line tuneable (UV and visible) argon ion laser. The lamp was of an on-axis design. The output passed a water filter to remove infrared radiation. Wavelength selection was by a 0.25 m monochromator with a grating blazed at 300 nm. The band-pass was set to 12 nm. Inspection with an analyzing polarizer showed that this arrangement gave unpolarized light. The output of the monochromator was focused onto the sample to give a rectangular cross section ca. 5 mm × 4 mm. For operation in the visible region, the discrete argon ion laser lines were separated by an intracavity prism. With UV optics, only multiline operation was achieved

and separation was extracavity. For polarization-resolved measurements, s- and p-polarized light was obtained using half wave plates optimized for 450 and 355 nm. This was not optimum for some lines, so the output was further processed by a polarizer set to pass s or p radiation. For both light sources, power measurement was by a calibrated thermoelectric detector.

The products of irradiation or heating were detected by a pulse-counting quadrupole mass spectrometer (Hiden HAL II 301 PIC) mounted on a translation stage. The mass spectrometer head was contained in a shroud with holes drilled to allow efficient pumping of the gas analyzer. The end of the shroud was conical with an access hole of 6 mm diameter. For temperature-programmed desorption (TPD) measurements, the entrance to the shroud was 3 mm from the surface. For measuring the flux of photodesorbed species during irradiation (photon-induced desorption, PID), the distance was increased to 9 mm to allow free access of the incident radiation and rotation of the sample for angle-resolved experiments. In all PID measurements, the error bars represent the range of two or three repeated measurements.

3. Results and Discussion

Temperature-programmed desorption measurements were made on the unirradiated surfaces to check their integrity. OCS adsorbs and desorbs molecularly, while the TPD of the NO-saturated Ag(111) surface shows both NO and N_2O desorption. These TPD spectra, which are presented elsewhere,[16] are in excellent agreement with those available in the literature.[7,14,19] This result gives confidence in the quality of the surfaces used here, since the desorption of N_2O in particular is very sensitive to the presence of surface defects.[16,19] The defect concentration on our surface was, by this yardstick, immeasurably small.

The TPD traces were also used to confirm the photochemical reaction. Post-irradiation TPD confirm that OCS photodissociates to yield S_a and CO_g. No S atoms were detected in the gas phase. For the NO-saturated surface, the observed photoproducts are NO and N_2O.[16a] The former arises from the dissociation of the NO dimer, while the latter arises either from a low-temperature N_2O adsorption site, or as a photoproduct of the NO dimer. These two reactions can be treated as separate, although there is some evidence for coupling between them.[7,16b]

The photochemical cross sections can be determined from an exponential fit to the measured PID traces if the photon flux is known.[1,20] Typical examples of the PID traces measured here are shown in Figure 3. The PID traces in Figure 3 are not strictly exponential, and this result was observed for NO and OCS data. These complex kinetics have their origin in the effect of photoproducts on the reaction rate and are discussed in more detail elsewhere.[16b] One effect of this behavior is to render the cross sections obtained from exponential fits to the data ambiguous. In the present case, where we are interested in only the relative photochemical cross section, as a function of polarization, wavelength, etc., the most accurate measurement will be the initial step size, proportional to the initial rate, in the PID, I_0, which is unaffected by product buildup.

The objective of the remainder of this section is to determine the primary excitation mechanism leading to the adsorbate photochemistry observed. NO, N_2O, and OCS do not exhibit strong electronic transition at wavelengths above 300 nm in the gas phase.[17] There are fewer studies of the NO dimer, the major surface species resulting from adsorption of NO on Ag(111),[15] but both experiment and recent calculations suggest negligible absorption in the 300−600 nm region.[18] Thus, the unperturbed electronic transitions of the adsorbates cannot contribute to the observed photochemistry. However, it is likely that the adsorbate's electronic structure is perturbed on adsorption, so electronic excitation of an adsorbate−substrate complex must be considered, along with the substrate-mediated hot electron attachment mechanism. These two mechanisms can in part be distinguished by polarization-resolved measurements, which are described next.

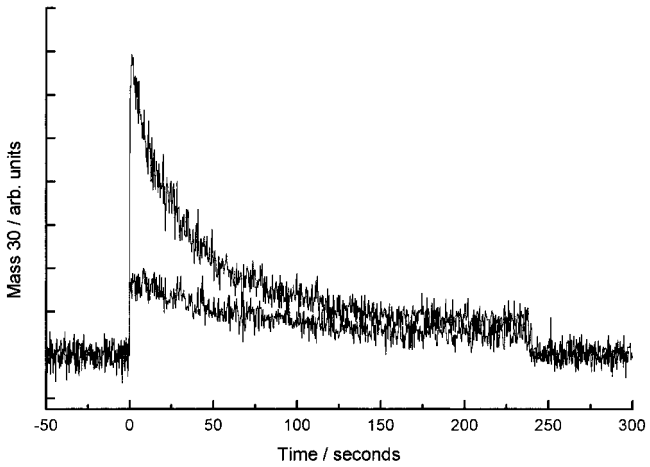

Figure 3. Illustration of the PID data recorded for the desorption of NO from Ag(111) on irradiation at 458 nm with an angle of incidence of 70°. The lower plot is for s-polarized radiation, and the upper for p-polarized radiation. The value of I_0 is taken from the intensity in the PID at $t = 0$.

3.1. Polarization-Resolved Measurements. Adsorbate- and substrate-mediated photochemistry can be distinguished by polarization and angle of incidence resolved studies of the initial rate of reaction. The calculations require as input the reflection coefficients for the perpendicular, r_s, and parallel, r_p, components of the electric vector of the incident radiation, which yield the reflectivity for s- and p-polarized light $R_p = |r_p|^2$ and $R_s = |r_s|^2$.[21,22] The reflection coefficients are functions of the angle of incidence, θ_i, and the optical constants of the metal, the refractive index, n_2, and the extinction coefficient, κ.[21,22] The optical constants have been tabulated for silver,[13] and the refractive index of the vacuum, n_1, is unity in all calculations.

For a primary mechanism involving the excitation of an adsorbate−substrate complex, the photochemical cross section will be proportional to $|\mu\cdot\mathbf{E}|^2$, where $\boldsymbol{\mu}$ is the transition dipole moment of the complex and $\mathbf{E}$ is the electric field of the incident radiation at the surface. For a beam incident on the surface in the *xz* plane, where *z* is the surface normal, the three components of $\mathbf{E}$ in the region of the interface can be calculated, within the limits of the classical theory, from[7,8,22]

$$\begin{aligned} E_x &= E_{ix}(1 - r_p)\cos\theta_i \\ E_y &= E_{iy}(1 + r_s) \\ E_z &= E_{iz}(1 + r_p)\sin\theta_i \end{aligned} \tag{1}$$

In eqs 1, the E_{ii} ($i = x, y, z$) are the incident optical fields in the *i* direction, which depend on the amplitude of the incident field E_0 and the polarization angle, ϕ, as $E_{iy} = E_0\cos\phi$ and $E_{ix} = E_{iz} = E_0\sin\phi$. Equations 1 can, after some assumptions are made about the adsorbate binding geometry, be employed to predict the polarization and angle of incidence dependence of photochemistry arising from an adsorbate excitation mechanism.[8] Conversely, for a substrate-mediated mechanism, it is the polarization and incidence angle dependence of the substrate absorption, *A*, which is of interest, which may be calculated

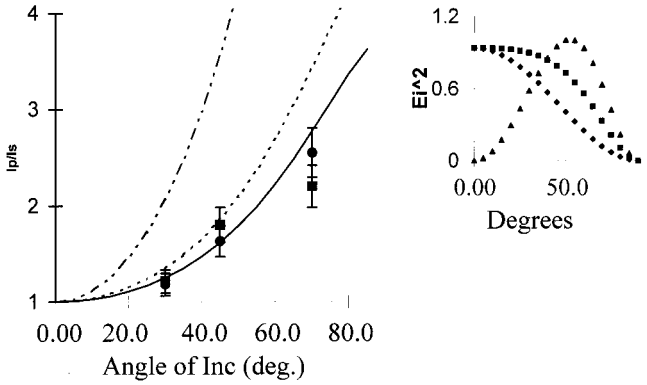

Figure 4. Ratio of I_0 measured for p- and s-polarized radiation for NO (■) and OCS (●) PID measured as a function of the angle of incidence. The data are compared with the predictions for adsorbate [with both an isotropic (− ·· −) and purely parallel (but isotropic in the surface plane) (- - -) orientation of the adsorbate transition dipole] and a substrate localized excitation (—); expressions for the different I_{0p}/I_{0s} are given in the text. Inset: the incident angle dependence of the square of the electric fields in the z (▲), y (◆), and x (■) directions.

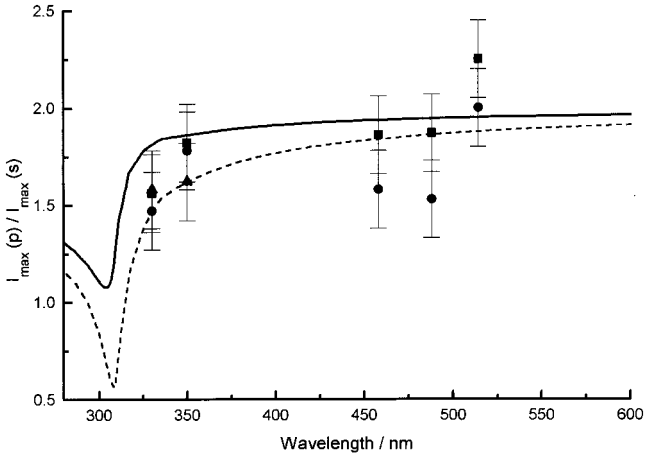

Figure 5. Ratio of I_0 calculated as in Figure 4, but data reported as a function of wavelength for a fixed incidence angle of 45°: NO (■); N_2O (●); OCS (▲). The model calculations are shown for (a) the substrate-mediated mechanism (solid line) and (b) a parallel adsorbate transition dipole (dashed line).

from

$$A = (1 - |r_s|^2)\cos^2\phi + (1 - |r_p|^2)\sin^2\phi \qquad (2)$$

Equations 1 and 2 have been employed in the analysis of several systems (including NO/Ag(111),[7] but not OCS/Ag(111)) to distinguish between the adsorbate- and substrate-mediated mechanisms. Most often a single wavelength has been used and the dependence of the cross section on θ_i or ϕ has been measured. For the present data, we compare the photochemical cross section, represented by the initial step size in the PID, I_0, measured with both s- and p-polarized radiation (I_{0p}/I_{0s}) as a function of both θ_i and the incident wavelength. The results are displayed in Figure 4 for the θ_i dependence and Figures 5 and 6 for the wavelength dependence (at the four argon ion laser wavelengths) at 30° and 70° angle of incidence, respectively.

For the adsorbate-mediated mechanism, three models for the orientation of the transition dipole $\boldsymbol{\mu}$ were considered.[8] First, for a transition dipole oriented along the surface normal, the prediction is that no photochemistry will be observed for s-polarized incident radiation. This is clearly in contradiction with

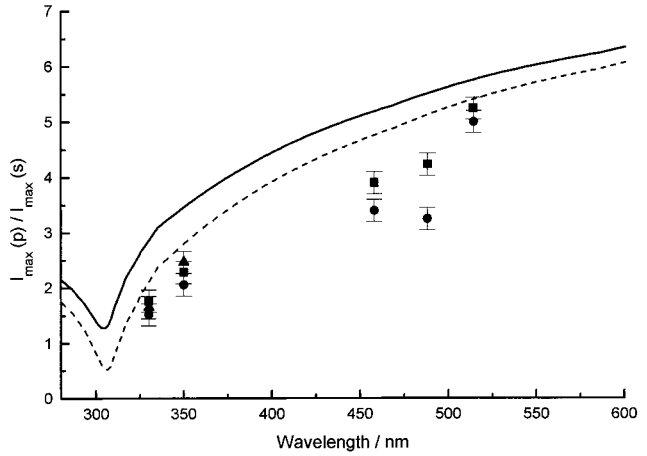

Figure 6. Ratio of I_0 calculated as in Figure 4, but data reported as a function of wavelength for a fixed incidence angle of 70°. Symbols same as for Figure 5.

experiment (see Figure 3) and may be discounted. Second, an isotropic distribution of the transition dipole predicts $(I_{0p}/I_{0s}) = (|E_x^2| + |E_z^2|)/|E_y^2|$, which is plotted in Figure 4. The agreement with the measured data is poor. Finally, for a transition dipole which is oriented parallel to the surface but isotropically distributed in the surface plane, $(I_{0p}/I_{0s}) = |E_x^2|/|E_y^2|$. This is shown in Figures 4−6, and the agreement between the data for all three adsorbates and the predictions of this particular adsorbate-mediated mechanism is reasonable. Turning to the substrate-mediated mechanism, it can be seen from eq 2 that $(I_{0p}/I_{0s}) = (1 - |r_s|^2)/(1 - |r_p|^2)$, which is also shown in Figures 4−6. This substrate-mediated mechanism is also seen to be in reasonably good agreement with the experimental data for all three adsorbates. Thus, these last two possibilities are not clearly distinguished by the polarization and angle of incidence dependence measurements, a fundamental difficulty with the polarization analysis already noted elsewhere.[23] However, the similarity between the results for OCS and NO does suggest that the same mechanism is operating in both adsorbates.

Unfortunately, the orientation of the adsorbate transition dipole relative to the surface normal is not known exactly in either case. For OCS on NaCl, adsorption is with the molecular axis parallel to the surface in a zigzag structure,[24] while on LiF-(001) OCS is adsorbed perpendicular to the surface with either S or O down in equal parts. This leads to the observation of both S and CO in the gas phase following photolysis at 222 nm, into the dissociative electronic transition of OCS.[25] The fact that no S atoms are observed in the gas phase on photolysis of the OCS/Ag(111) system certainly suggests bonding through the S atom, and work function change measurements support this configuration.[14] Such a "sulfur down" configuration would suggest at least a component of the transition dipole vector in the z direction. However, there is no evidence of this from the data of Figures 4−6, although the measurement of I_p/I_s is sensitive to a component of $\boldsymbol{\mu}$ in the z direction, especially at higher angles of incidence. For NO, which exists as the dimer on Ag(111), the adsorbate geometry has been determined by vibrational spectroscopy.[15] The cis dimer is of C_{2v} symmetry and is formed by a weak N−N bond which lies parallel to the surface. The dimer is planar and is slightly tilted (about 30°) from the surface normal.[26] However, since electronic spectra of the dimer are scarce, it is difficult to speculate on the direction of the transition dipole in the adsorbate. It is then only possible to conclude from the data of Figures 4−6 that either (i) the primary photochemical mechanism is substrate-mediated hot

electron attachment or (ii) that an adsorbate-mediated mechanism operates and that, somewhat surprisingly, the transition dipoles of all adsorbates lie wholly parallel to the surface (since a significant perpendicular component in $\boldsymbol{\mu}$ would easily be observed because of the large value of E_z^2 at the values of θ_i used; see Figure 4).

One further conclusion can be drawn from the wavelength-dependent data of Figures 5 and 6. They do not reveal any evidence for a switch from a substrate-mediated to an adsorbate-mediated mechanism at shorter wavelengths. The adsorbate-mediated (or parallel transition dipole) mechanism is equally good at all wavelengths for both OCS and NO. So et al.[7] suggested a change of mechanism from substrate- to adsorbate-mediated at around 400 nm for NO photodesorption from Ag(111). This was introduced to account for the observed deviation of the action spectrum for photochemistry from that predicted on the basis of substrate absorption. An analysis of the action spectrum for OCS and NO photochemistry is the topic of the next section.

3.2 Action Spectra. While the polarization- and angle-resolved measurements described above can, in principle, distinguish between the two primary mechanisms of adsorbate photochemistry, they have the limitation that the absolute absorption intensity is divided out in the result. This means that the measurement is insensitive to the (presumably different) wavelength dependence of the substrate and adsorbate absorption cross sections. A measurement of the relative photochemical cross section as a function of the incident wavelength should therefore be a superior method of distinguishing between the two primary mechanisms.[1,7]

The absorption of the Ag(111) substrate for unpolarized light is given by $(1 - R_{eff})$ where $R_{eff} = (R_s + R_p)/2$. The wavelength dependence can be obtained from the frequency-dependent optical constants of silver.[13,22] The resulting absorption profile is strongly peaked around 320 nm (Figure 7a). This peak is not observed in the measurements (see below) but, as first pointed out by Ho and co-workers,[7] the probability of hot electron attachment is proportional to the number of hot electrons generated by absorption which ultimately reach the surface. Thus, the simple absorption profile must be corrected to account for the penetration depth of radiation and the mean free path of the hot electron; hot electrons generated deep in the substrate are less likely to reach the surface. Thus, the effective absorbance is

$$A(\lambda) = (1 - R_{eff}(\lambda))(1 - e^{-\alpha(\lambda)\Lambda}) \qquad (3)$$

in which $\alpha(\lambda)$ is the wavelength-dependent absorption coefficient of the metal[7,8,21,22] and Λ is the electron mean free path. In general, Λ is also wavelength dependent, but in the relatively narrow energy range of interest here it can be taken to be of the order of 10 nm.[7] The resultant $A(\lambda)$, Figure 7b, is a much smoother function of wavelength, as has been shown previously by So et al.[7] Of course, no such correction is required for the electric field experienced by the adsorbate, eqs 1, so these retain the sharply peaked form, shown in Figure 7a. In Figure 7b, the initial step sizes, I_0, in the PID traces, recorded with unpolarized light, are shown as a function of wavelength for CO, NO, and N_2O desorption from irradiated OCS- and NO-saturated Ag(111). Also shown is a plot of eq 5, the corrected absorbance of the substrate.

The photochemical action spectra for all three adsorbates on Ag(111) reveal remarkable similarities, in particular in the monotonically increasing cross section for wavelengths below 380 nm. This similarity is in itself a rather persuasive argument

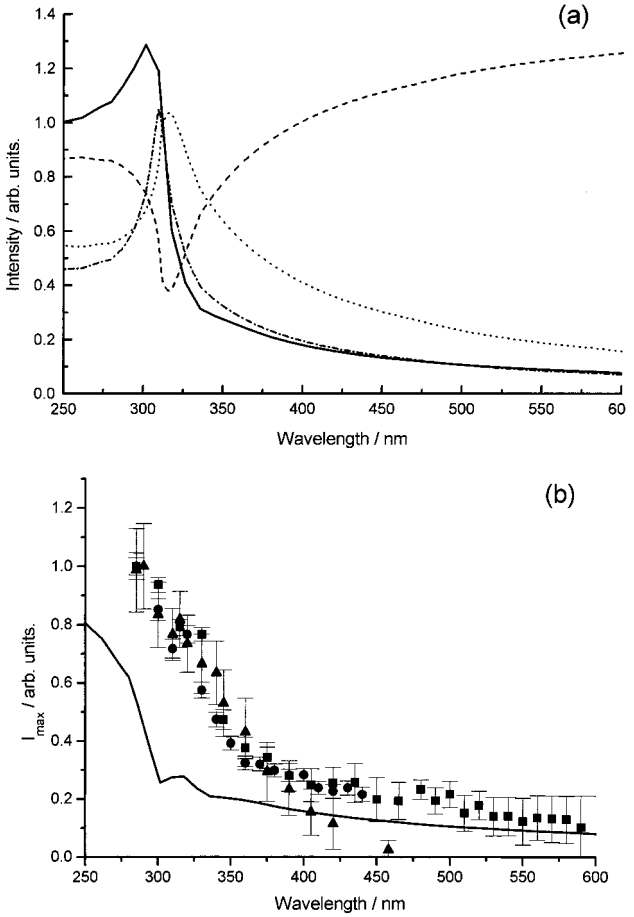

Figure 7. (a) Predictions of the classical model for the interpretation of action spectra. The three electric fields experienced by the adsorbate are shown (eqs 1, E_z (- - -), E_x (···), E_y (· − ·) along with the calculated substrate absorbance (eq 2, −). Note that the absorbance and the in-plane electric fields all exhibit sharp peaks at around 300−320 nm. (b) Action spectra for all three adsorbates, NO (squares), N_2O (circles), and OCS (triangles). Also shown is the action spectrum predicted by the effective substrate absorbance, determined from eq 3.

in support of the operation of a substrate-mediated mechanism, since both the photochemical reactions, the electronic structure, and the bonding interaction with the surface are different for the two adsorbates. Thus, an adsorbate-mediated process would be expected to reveal rather different action spectra for the two adsorbates. In addition, if an adsorbate-mediated mechanism (which must, according to the polarization-resolved data of Figures 4−7, involve a transition dipole parallel to the surface) makes an important contribution to the action spectrum, a peak around 320 nm would be predicted, since both parallel components of the electric field above the surface peak at this wavelength (Figure 7a). That this is not observed is again evidence against the operation of an adsorbate mediated mechanism.

It should also be noted that the data are not particularly well described by the simplest model for a substrate-mediated mechanism, eq 3 (see Figure 7b). For wavelengths shorter than 350 nm, the measured increase in cross section exceeds considerably that predicted by eq 3. A similar deviation was noted by So et al. for the NO/Ag(111) (and Cu(111)) system and ascribed to the operation of an adsorbate-mediated pathway at higher energy.[7] However, the polarization-resolved data of Figures 5 and 6 do not suggest a change in mechanism with decreasing wavelength. A second deviation from eq 3 can also be seen at longer wavelength. While NO (and N_2O) photode-

sorption certainly takes place up to at least 600 nm, Figure 7b reveals a cut-off wavelength for OCS photodissociation. The CO desorption signal is not resolvable at wavelengths longer than 500 nm. The failure of eq 3 to describe quantitatively the measured action spectra suggests that the substrate absorption−HEA model outlined above needs to be further modified. The most obvious factor missing from the model is a consideration of the electronic structure of the adsorbate.

The essential features of the substrate excited HEA model were presented in Figure 1. The wavelength-dependent probability of inducing an adsorbate reaction is a convolution of three energy-dependent factors: the hot electron distribution at the surface; the electron tunneling probability; the electron attachment levels of the adsorbate.[12] The distribution of hot electrons available for attachment, $S(E_e,h\omega)$, includes both the nascent distribution, which extends from E_F up to the energy of the incident photon, and the distribution of secondary or scattered electrons. Following the discussion of Weik et al., this distribution is given approximately by[11]

$$S(E_e,h\omega) \propto \frac{A(h\omega)}{h\omega}\left(\frac{h\omega}{E_e}\right)^{\beta}\Phi(h\omega - E_e) \qquad (4)$$

In eq 4, $A(h\omega)$ is the effective substrate absorption (eq 3), $h\omega$ is the photon energy, E_e is the electron energy, β is a constant (equal to 1 if only the nascent distribution is important), and $\Phi(h\omega - E_e)$ is the Heaviside function. The other factor which is important in determining the form of the action spectrum, the convolution of the adsorbate attachment level with the barrier to electron tunneling, has been discussed by Harris et al.[12] These authors find that the yield for electron attachment as a function of electron energy can be represented by a skewed Gaussian which is peaked to slightly higher energy than the attachment level of the adsorbate. The overall energy dependence is not a strong function of barrier width,[12] so in our model calculations this will be approximated by a simple Gaussian function, $Y_0(E_e)$. It should be noted that the absolute reaction yield does depend strongly on the barrier width, increasing with increasing width due to the longer lifetime of the affinity level, up to a limit where the increasing width prevents electron attachment and the yield falls.[12] This effect of barrier width on the absolute yield can be neglected when comparing results at different wavelengths. Thus, the total yield for HEA-induced adsorbate chemistry, $Y_0(h\omega)$, will be modeled here by the convolution[12]

$$Y_0(h\omega) = \int_{E_F}^{\infty} Y_0(E_e)S(E_e,h\omega)\,dE_e \qquad (5)$$

where $Y_0(E_e) = (1/\sqrt{2\pi}s)\exp(-(E_{max} - E)^2/2s^2)$ is a Gaussian peaked at E_{max} of width ΔE, where $s = \Delta E(8 \ln 2)^{-1/2}$, where E_{max} is an energy slightly in excess of the energy of the adsorbate electron attachment level.

Unfortunately, there is little data available on the electronic structure of adsorbates. Hence, the data of Figure 7b will first be analyzed within the limits of the above model, making assumptions about the energies of the attachment levels, and then the electronic structure assumed will be discussed in relation to what is known about the gas-phase electron attachment levels of NO and OCS.

Taking OCS first, the action spectra are well fit under the assumptions that $Y(E_e)$ has E_{max} at 3.2 eV with a width 0.8 eV. The action spectrum is then described in terms of eqs 3−5. The fit is shown in Figure 8 with $\beta = 1$, i.e., the nascent hot electron distribution. Inclusion of the secondary electron distribution does not improve the fit. This is the result expected from the calculations of Hellsing and Zhdanov who found, in line with a qualitative expectation, that secondary electrons make a more significant contribution for attachment levels close to E_F.[27]

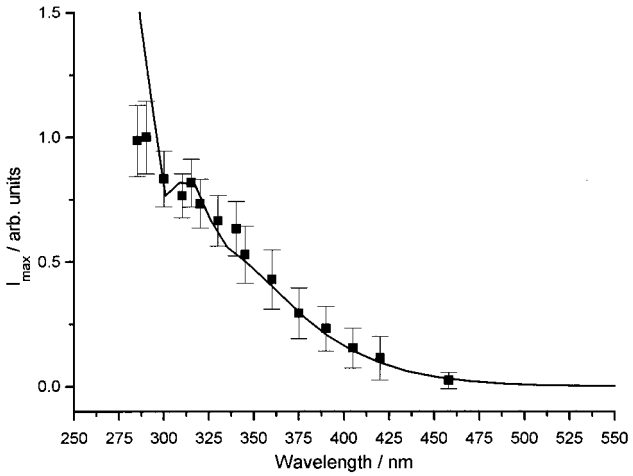

Figure 8. Action spectrum for the dissociative desorption of CO from OCS/Ag(111). In the calculation (solid line), a dissociative electron attachment level at 3.2 eV has been assumed. See text for discussion.

The question naturally arises, is there a justification for the assumption of an attachment level 3.2 eV above E_F? Iga and co-workers have investigated the dissociative electron attachment of OCS in the gas phase.[28] They measured the yield of S^- as a function of incident electron energy using a time-of-flight method. An intense resonance peaked at 1.4 eV was observed, with an onset at 0.4 eV and a second weaker resonance at 4.7 eV with an onset at 3.9 eV. It was suggested that dissociation occurred via a $^2\Pi$ negative ion resonance of OCS in the former case and $^2\Delta$ in the latter. These data are consistent with the dissociation of OCS in the adsorbed state being induced by hot electron attachment. The energies of electron attachment levels are conventionally referenced to the vacuum level, while the photoexcited hot electron energy is referenced to the E_F. Clearly then there is insufficient energy in the incident photons to access these levels if they are unperturbed by the surface. However, the energies of negative ion states are strongly perturbed by adsorption onto a surface. On a metal surface, the image charge stabilization energy alone can lower the energy by ~2 eV.[29] This would bring the lowest energy gas-phase negative ion resonance of OCS below the vacuum level (the work function for Ag(111) covered with a monolayer of OCS was measured as 4.1 eV[14]) and in range of hot electrons generated by 400 nm (~ 3 eV) photons. Thus, dissociative electron attachment to adsorbed OCS in the energy region of 3.2 eV is certainly plausible.

It would, however, be wrong to definitively identify the energy level assumed in the fit of Figure 7 with a particular level in the gas-phase spectrum. There are strong perturbations to the energy of negative ion states on adsorption, in addition to image charge attraction. This will be particularly true when there is a degree of chemisorption leading to structural changes in the adsorbate.[30] The observation and understanding of the energetics of negative ion states in adsorbates is one of the most important unsolved problems in interpreting surface photochemistry.

Turning now to the NO case, the action spectrum for photodesorption was fit in terms of eqs 3−5. A good fit required a high- and a low-energy attachment level. For the fit shown in Figure 9, E_{max} = 3.9 eV, width 0.5 eV, and E_{max} = 1.2 eV, width 1.0 eV, were assumed. The fit is shown in Figure 9, which reveals a significant effect of secondary electron attachment (β

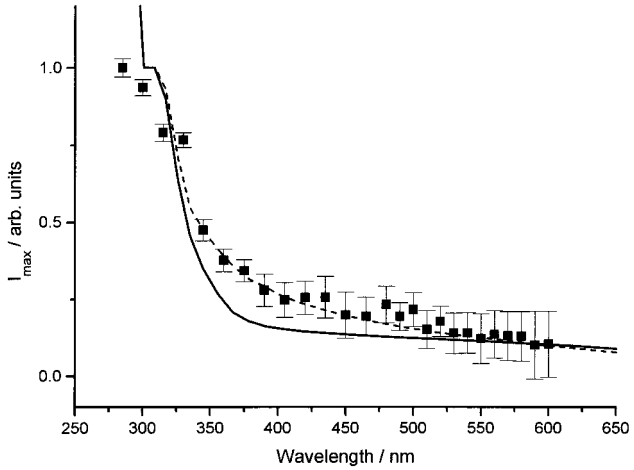

Figure 9. Action spectrum for the desorption of NO from Ag (111). The calculation assumes two attachment levels at 1.0 and 3.9 eV. If the effects of secondary electrons are neglected, the solid line results, while their inclusion leads to the good fit indicated by the dashed line. If only a single attachment level is assumed, the entire data set cannot be fit, even when electron cascades are invoked.

$= 1.6$). A significant role for secondary electrons is expected because of the low energy of one of the attachment levels.[27] Such a low-energy attachment level is required to reproduce the tail in the action spectrum which extends beyond 600 nm. Attempts were made to fit the entire curve with a single low-energy attachment level and varying values of β, but it was not possible to reproduce the rapid rise in cross section observed around 350 nm. Hence the second high-energy attachment level is required to fit the data.

The electronic structure of adsorbed NO has been studied in some detail.[31] For the particular case of Cu(111), Kinoshita et al. found in two photon photoemission experiments a negative ion state 1.2 eV above the Fermi level and a second resonant transition at 3.9 eV.[32] These results guided the choice of $Y_0(E_e)$ in the above analysis. However, the result of ref 32 cannot be taken over directly into the hot electron attachment analysis, since the 3.9 eV transition was assigned to an adsorbate-localized one. This is consistent with the proposition of So et al. for the NO/Cu(111) photodesorption mechanism at wavelengths below 350 nm[7] but is in contrast to the polarization analysis presented above for the Ag(111) surface, which suggested a substrate excitation mechanism (Figures 4−6). These two results are only compatible if the transition dipole associated with the 3.9 eV transition is oriented parallel to the surface. In that case, the similarity of the NO photodesorption action spectrum with that for OCS photodissociation (Figure 7b) is simply a coincidence. Further, excitation of an adsorbate resonance peaked at 3.9 eV would predict a decrease in the photodesorption cross section on irradiation at higher energy. The data of Figure 9 do not show such a turnover, at least up to 4.3 eV, the limit of our measurement. An alternative explanation for the good fit to the data shown in Figure 9 is that there is in fact an accessible negative ion state >3 eV above the Fermi level on the Ag(111) surface, as assumed in the analysis; there is, however, no experimental data to support such an assignment.

In this analysis of the NO action spectrum, we have not taken into account the complex multicomponent nature of the surface that results from exposure of Ag(111) to NO.[7,15,16a] The significance of this complexity for the photokinetics is discussed elsewhere,[16b] but one important conclusion is that the photoactive species is the NO dimer.[15,16] The NO dimer does not have any optical transitions in the 300−500 nm range[18] but does exhibit dissociative electron attachment (to NO and NO^-) at very low electron energies.[33] Thus, the HEA mechanism outlined above for NO photodesorption from Ag(111) remains plausible when the dimeric nature of the adsorbed species is taken into account.

The composite nature of the NO on Ag(111) surface also complicates the analysis of the N_2O photodesorption. As seen in Figure 7b, and noted earlier by So et al.,[7] the action spectrum for N_2O exactly mirrors that for NO. Thus, the action spectrum can be simulated with the same parameters for attachment levels as were used for NO. However, the gas-phase negative ion data for N_2O are more similar to those of OCS than NO, exhibiting a low-energy (dissociative) attachment level at around 1−3 eV.[34] When the effect of image charge stabilization is taken into account, it is likely that HEA can account for the desorption induced by UV photons. That photodesorption rather than photodissociation is observed is not in conflict with the HEA mechanism. It is possible that dynamics on the dissociative surface simply cannot compete with those of the desorption and quenching channels indicated in Figure 1. Other groups have found that N_2O on Pt(111) exhibits both photodissociation and photodesorption,[35] Masson et al. also proposed that competition between dissociative and desorption pathways occurs.[35c] It is more difficult to understand the low-energy photodesorption of N_2O. The similarity of the action spectra for NO and N_2O might suggest that the two desorption channels are coupled, i.e., that one photochemical pathway for the NO dimer is photosynthesis of N_2O

$$(NO)_{2,a} \rightarrow N_2O_g + O_a$$

There is some evidence for this in the photokinetics.[16b] On the other hand, the TPD data show photodesorption of N_2O takes place from a single low-temperature site, suggesting separate channels.[16,17]

We conclude this section with some observation on alternative mechanisms. Above, the focus has been on hot electron attachment. It has been shown that this mechanism may be consistent with the rapid rise in cross section observed at wavelengths below 350 nm for both adsorbates if some assumptions are made about the energies of the electron attachment level(s) of the adsorbates. One alternative mechanism which should be considered is the effect of a substrate-localized transition on the adsorbate bond.[36] At around 3.8 eV, the excitation of the silver d band to E_F transition occurs. It is at least a possibility that, if these d band electrons were involved in bonding interactions with the adsorbate, then their excitation might also contribute to adsorbate photochemistry. Such a mechanism has recently been invoked in an analysis of the photodesorption dynamics of NO from Pt(111).[36] This mechanism would lead to substrate-mediated photodesorption, consistent with the polarization analysis, and predict an onset around 350 nm, consistent with the rising part of the action spectra. However, such a resonant substrate excitation mechanism cannot explain all of the data. First, a maximum in the action spectrum would be predicted at around 320 nm, which is not observed. Second, it is not clear how such a substrate-localized excitation could lead to the dissociation of OCS. Finally, we note that Howe and Dai have very recently proposed an alternative mechanism for photodesorption of weakly bound adsorbates.[37] They suggested that adsorbate vibrational excitation can occur as a result of substrate excitation through a dipole mechanism. The subsequent vibrational relaxation may cause dissociation of the physisorption bond. The threshold energy for this

mechanism would be very low, in the IR region. Such a mechanism could account for the long-wavelength desorption of NO and N_2O (Figure 7). For NO, vibrational excitation could lead to dissociation of the weak N−N bond of the dimer. This mechanism would be consistent with substrate excitation demonstrated above. The signature of this mechanism is a low translational energy in the photoproduct.[37] Such dynamical measurements, as well as further work on the efficiency of the vibrational excitation process, are required to test further this mechanism.

4. Summary and Conclusions

The photochemistry of two adsorbates which exhibit quite different photoreactions has been compared on a common substrate. For NO-saturated Ag(111), irradiation yields both NO and N_2O. The former arises from the dissociation of the NO dimer, while the latter arises from direct photodesorption and/or photosynthesis. On the other hand, OCS adsorbs molecularly on Ag(111) and undergoes photodissociation to yield CO and adsorbed S. The photokinetics of these adsorbates are described further in a companion paper[16b] the focus of this work was on the primary mechanism of photochemistry.

The photochemical yield has been studied for both s- and p-polarized radiation at wavelengths between 334 and 514 nm. The data were compared with the predictions of classical models for photochemistry induced by the incident field above the surface (adsorbate mediated) and for photochemistry induced by substrate absorption. For both adsorbates at all wavelengths studied, the photochemistry was equally well described by substrate excitation or absorption by an adsorbate-localized transition oriented exclusively parallel to the surface. An adsorbate-mediated mechanism therefore requires that neither OCS nor the NO dimer have any component of their transition dipole moments perpendicular to the surface.

The photochemical yield was measured as a function of wavelength (action spectrum) with unpolarized light. Remarkable similarities between the action spectra were found for the two adsorbates, consistent with a substrate-mediated mechanism. In both cases, the action spectra rose monotonically between 400 and 280 nm. For OCS, there is a cut-off wavelength at 500 nm, while NO and N_2O desorption occurs up to at least 600 nm. The action spectra were also analyzed in terms of the classical models for adsorbate- and substrate-mediated mechanisms. Calculations for the adsorbate-mediated mechanism predicted a peak in the cross section at 320 nm, which was not observed. The calculation for the substrate-mediated mechanism predicts a smoothly rising curve, but the rate of increase at wavelengths below 350 nm is not sufficiently large to fit the data (Figure 7b).

The data were further analyzed in terms of a model for substrate-mediated hot electron attachment, including the effects of secondary electrons and the energies of adsorbate electron attachment levels. It was noted that the attachment levels are in general unknown, so some assumptions are required.

For OCS, the data were well reproduced by assuming an attachment level 3.2 eV above E_F. The simulation required only the nascent population of hot electrons, consistent with the idea that secondary electrons will make their most significant contribution for attachment levels well below the photon energy and close to E_F. Gas-phase OCS has dissociative electron attachment levels at energies above 0.4 eV. With image charge stabilization, this would be in reasonable agreement with the energy level assumed. However, in the case of OCS, there is weak bonding to the surface which will certainly perturb the attachment levels relative to the gas phase, thus to identify the assumed level with the gas-phase level is a severe approximation. To go further requires direct electronic structure measurements on the adsorbed molecule.

For NO/Ag(111), two attachment levels had to be assumed to reproduce the action spectra, located at 1.2 and 3.9 eV. Hot electron cascades also had to be included in the calculation. The energy levels assumed are consistent with the two photon photoemission data of Kinoshita et al.[32] However, the 3.9 eV transition was assigned by Kinoshita et al. to an adsorbate-localized one, not an electron attachment level as assumed here. Thus, the 3.9 eV level assumed has not been observed experimentally. It was not possible to provide a more detailed rationalization of the attachment levels assumed for NO (and N_2O). This problem probably arises from the complex multicomponent nature of the NO/Ag(111) surface.

In conclusion, the photochemistry of two rather different adsorbates on the same surface revealed many similarities. All the data were consistent with a substrate-mediated hot electron attachment mechanism. However, quantitative simulation required assumptions to be made about the electronic structure of the adsorbate. For a definitive test of the model, new experimental measurements of adsorbate electron attachment levels are required.

Acknowledgment. We are grateful to EPSRC for financial support. R.T.K. thanks EPSRC for a postgraduate studentship.

References and Notes

(1) (a) Zhou, X.-L.; Zhu, X.-Y.; White, J. M. *Surf. Sci. Rep.* **1991**, *13*, 76. (b) Ho, W. In *Laser Spectroscopy and Photochemistry on Metal Surfaces*; Dai, H.-L., Ho, W., Eds.; World Scientific: Singapore, 1995; p 1047. (c) Meech, S. R.; Kidd, R. T. In *Specialist Periodical Report, Photochemistry*; Gilbert, A., Ed.; Royal Society of Chemistry: London, 1997; Vol. 28, p 465. (d) Meech, S. R. In *Specialist Periodical Report, Photochemistry*; Gilbert, A., Ed.; Royal Society of Chemistry: London, 1992; Vol. 23, p 479. (e) Zimmerman, F. M.; Ho, W. *Surf. Sci. Rep.* **1995**, *22*, 195. (f) Ho, W. *Surf. Sci.* **1994**, *299/300*, 996.

(2) The general form of the potential energy surfaces used in the calculation of photon and/or electron stimulated desorption are described in the following: Antoniewicz, P. R. *Phys. Rev. B.* **1980**, *21*, 3811. Menzel, D. Gomer, R. *J. Chem. Phys.* **1964**, *41*, 3311. Redhead, P. A. *Can. J. Phys.* **1964**, *42*, 886. Menzel, D. *Nucl. Instrum. Methods Phys. Res., Sect. B* **1995**, *101*, 1.

(3) (a) Richter, L. T.; Buntin, S. A.; Cavanagh, R. R.; King, D. S. *J. Chem. Phys.* **1988**, *89*, 5344. (b) Buntin, S. A.; Richter, L. T.; Cavanagh, R. R.; King, D. S. *Phys. Rev. Lett.* **1988**, *61*, 1321. (c) Ferm, P. M.; Budde, F.; Hamza, A. V.; Jakubith, S.; Ertl, G.; Weide, D.; Andresen, P.; Freund, H. J. *Surf. Sci.* **1989**, *218*, 467. (d) Richter, L. T.; Buntin, S. A.; Cavanagh, R. R.; King, D. S. *J. Chem. Phys.* **1992**, *96*, 2324.

(4) (a) Gadzuk, J. W.; Richter, L. T.; Buntin, S. A.; Cavanagh, R. R.; King, D. S. *Surf. Sci.* **1990**, *235*, 317. (b) Gadzuk, J. W. *Surf. Sci.* **1995**, *342*, 345. (c) Gadzuk, J. W. In *Femtosecond Chemistry*; Manz, J., Woste, L., Eds.; Springer: Berlin, 1994. (d) Guo, H.; Chen, F. *Faraday Discuss.* **1997**, *108*, 309. (e) Saalfrank, P.; Holloway, S.; Darling, G. R. *J. Chem. Phys.* **1995**, *103*, 6720. (f) Guo, H.; Seideman, T. *J. Chem. Phys.* **1995**, *103*, 9062.

(5) Hasselbrink, E. *Appl. Surf. Sci.* **1994**, *79/80*, 34.

(6) (a) Ying, Z. C.; Ho, W. *J. Chem. Phys.* **1991**, *94*, 5701. (b) Matsumoto, Y.; Grudzkov, Y. A.; Watanabe, K.; Sawabe, K. *J. Chem. Phys.* **1996**, *105*, 4775. (c) Zhu, X.-Y.; White, J. M. *J. Chem. Phys.* **1991**, *94*, 1555.

(7) So, S. K.; Franchy, R.; Ho, W. *J. Chem. Phys.* **1991**, *95*, 1385.

(8) Zhu, X.-Y.; White, J. M.; Wolf, M.; Hasselbrink, E.; Ertl, G. *Chem. Phys. Lett.* **1991**, *176*, 459.

(9) Ho, W. In Laser Spectroscopy and Photochemistry on Metal Surfaces; Dai, H.-L., Ho, W., Eds.; World Scientific: Singapore, 1995; p 1082−3.

(10) (a) Cemic, F.; Kolasinski, K. W.; Hasselbrink, E. *Chem. Phys. Lett.* **1994**, *219*, 113. (b) Hellsing, B. *Surf. Sci.* **1993**, *282*, 216. (c) Xin, Q.-S.; Zhu, X.-Y. *Surf. Sci.* **1996**, *347*, 346.

(11) Weik, F.; de Meijere, A.; Hasselbrink, E. *J. Chem. Phys.* **1993**, *99*, 682.

(12) Harris, S. M.; Holloway, S.; Darling, G. R. *J. Chem. Phys.* **1995**, *102*, 8235.

(13) Weaver, J. H.; Krafka, C.; Lynch, D. W.; Koch, E. E. *Physics Data, Optical Properties of Metals, Part II*; Fach-Informations-zentrum: Karlsruhe, 1981.

(14) Zhou, X.-L.; White, J. M. *Surf. Sci.* **1990**, *235*, 259.

(15) Brown, W. A.; Gardner, P.; King, D. A. *J. Phys. Chem.*. **1996**, *99*, 7065.

(16) (a) Kidd, R. T.; Lennon, D.; Meech, S. R. *Chem. Phys. Lett.* **1996**, *262*, 142. (b) Kidd, R. T.; Lennon, D.; Meech, S. R. In Preparation.

(17) Okabe, H. *Photochemistry of Small Molecules*; Wiley: New York, 1978.

(18) (a) Billingsley, J.; Callear, A. B. *Trans. Faraday Soc.*. **1971**, *67*, 589. (b) Mason, J. *J. Chem. Soc., Dalton Trans.* **1975**, 19. (c) East, A. L. L. *J. Chem. Phys.* **1998**, *109*, 2185.

(19) Jansch, H. J.; Huang, C.; Ludviksson, A.; Rocker, G.; Redding, J. D.; Metiu, H.; Martin, R. M. *Surf. Sci.* **1989**, *214*, 377.

(20) Guo, X.; Yoshinobu, Y.; Yates, J. T., Jr. *J. Chem. Phys.* **1990**, *92*, 4320.

(21) Jenkins, F. A.; White, H. E. *Fundamentals of Optics*, 4th ed.; McGraw-Hill: New York, 1981.

(22) Born, M.; Wolf, E. *Principles of Optics*, 6th ed.; Pergamon: Elmsford, NY, 1980; Chapter 13.

(23) Richter, L. J.; Buntin, S. A.; King, D. S.; Cavanagh, R. R. *Chem. Phys. Lett.* **1991**, *186*, 423.

(24) Picaud, S.; Girardet, C.; Glebov, A.; Toennies, J. P.; Dohrman, J.; Weiss, H. *J. Chem. Phys.* **1997**, *106*, 5271.

(25) Leggett, K.; Polanyi, J. C.; Young, P. A. *J. Chem. Phys.* **1990**, *93*, 3645.

(26) Brown, W. A.; Gardner, P. A.; Perez-Jigato, M.; King, D. A. *J. Chem. Phys.* **1995**, *102*, 7277.

(27) (a) Hellsing, B.; Zhdanov, V. P. *Photochem. Photobiol. A: Chem.* **1994**, *79*, 221. (b) Hellsing, B.; Zhdanov, V. P. *J. Electron. Spectrosc. Relat. Phenom.* **1993**, *64/65*, 563.

(28) Iga, A.; Srivastava, S. K. *J. Mol. Struct., (THEOCHEM)* **1995**, *335*, 31.

(29) Rous, P. J. *Surf. Sci.* **1992**, *260*, 361.

(30) Cemic, F.; Dippel, O.; Hasselbrink, E.; Palmer, R. E. *J. Chem. Soc., Faraday Trans.* **1995**, *91*, 3633.

(31) (a) Avouris, Ph.; DiNardo, N. J.; Demuth, J. E. *J. Chem. Phys.* **1984**, *80*, 491. (b) Johnson, P. D.; Hubert, S. L. *Phys. Rev. B* **1987**, *35*, 9427. (c) Edamoto, K.; Maehara, S.; Miyahara, E.; Miyahara, T.; Kato, H. *Surf. Sci.* **1988**, *204*, L739.

(32) Kinoshita, A.; Misu, A.; Munakata, T. *J. Chem. Phys.* **1995**, *102*, 2970.

(33) Christophorou, L. G. *Atomic and Molecular Radiation Physics*; Wiley: London, 1976; p 466.

(34) Bass, A. D.; Lezius, M.; Ayotte, P.; Parenteau, L.; Cloutier, P.; Sanche, L. *J. Phys. B: At. Mol. Opt. Phys.* **1997**, *30*, 3527 and references therein.

(35) (a) Kiss, J.; Lennon, D.; Jo, S. K.; White, J. M. *J. Phys. Chem.* **1991**, *95*, 8054. (b) Sawabe, K.; Matsumoto, Y, K.; Lee. J. *J. Chem. Phys.* **1993**, *99*, 3143. (c) Masson, D. P.; Lanzendorf, E. J.; Kummel, A. C. *J. Chem. Phys.* **1995**, *102*, 9096.

(36) Guo, H.; Chen, F. *Faraday Discuss.* **1997**, *108*, 309.

(37) Howe, P.-T.; Dai, H.-L. *J. Chem. Phys.* **1998**, *108*, 7775.